

1976), p. 413, and *Solid State Commun.* **18**, 831 (1976).
²⁷T. L. Reinecke, A. K. Ganguly, and K. L. Ngai,
Solid State Commun. **24**, 785 (1977); K. L. Ngai and

T. L. Reinecke, *Phys. Rev. B* **16**, 1077 (1977), and
 references therein.

²⁸See, e.g., R. N. Bhatt, *Phys. Rev. B* **17**, 2947 (1978).

Charged Particles in Polarizable Fluids

E. L. Pollock and B. J. Alder

Lawrence Livermore Laboratory, University of California, Livermore, California 94550

(Received 28 April 1978)

A molecular-dynamics calculation of the work of introducing a charge in a polarizable fluid leads to about twice the value predicted by the Born continuum model. The screened Coulomb field reaches its macroscopic limit about three molecular diameters from the charge but is larger than the continuum dielectric prediction because of higher-order polarizability corrections. The diffusion coefficient leads to a Stokes radius that corresponds roughly to a singly ionized particle and its solvation shell diffusing as a unit.

Despite the importance of solutions of electrolytes in many physical and particularly biophysical situations it is remarkable that primary reliance for estimating both equilibrium and transport properties of such systems is still based on continuum models.^{1,2} Recently several works concerned with ion dynamics in polar fluids have appeared, but these present either continuum models³ or an heuristic approach⁴ to account for relaxation of the solvent as the ion moves through it. In hopes of stimulating the development of molecularly based statistical-mechanical theories for these systems and to check on the accuracy of continuum-model predictions, we present here a molecular-dynamics study of a charged particle in an idealized solvent consisting of point polarizable atoms.

The model is defined by the potential-energy function

$$U = -q \sum_i \vec{p}_i \cdot \frac{\vec{r}_{i0}}{r_{i0}^3} - \sum_{i>j} \vec{p}_i \cdot \vec{T}_{ij} \cdot \vec{p}_j + \sum_i \frac{P_i^2}{2\alpha} + \sum_{i>j} V(r_{ij}). \quad (1)$$

The first term describes the interaction of the charge, q , of the nonpolarizable particle, 0, with the induced dipoles, \vec{p}_i . The second term represents the induced-dipole-induced-dipole interaction via the dipole tensor $\vec{T} = \nabla\nabla(1/r)$. The third term is the potential energy of induced-dipole formation, where α is the isotropic point polarizability of the solvent particles. Finally, the last term represents the pairwise short-range interaction between all particles including the charged particle. For this the Lennard-Jones 12-6 potential was used with the well depth at $r = 2^{1/6}\sigma$

denoted by ϵ_{LJ} to avoid confusion with the dielectric constant ϵ . The induced polarization at particle i is proportional to the instantaneous electric field at i ,

$$\vec{p}_i = \alpha \vec{E}_i = \alpha [q(\vec{r}_{i0}/r_{i0}^3) + \sum_j \vec{T}_{ij} \cdot \vec{p}_j]. \quad (2)$$

In the computations the electric field at i is obtained iteratively from Eq. (2) using the value of \vec{p}_i at the preceding step. If the iteration is started from the polarization due to the pure Coulomb field of the charged particle, the terms in the expansion in powers of α for

$$\vec{E}_i = q \frac{\vec{r}_{i0}}{r_{i0}^3} + \alpha q \sum_{j \neq i} \vec{T}_{ij} \cdot \frac{\vec{r}_{j0}}{r_{j0}^3} + O(\alpha^2) \quad (3)$$

can be examined separately.

The linear term in Eq. (3) is correctly given by the dielectric continuum theory when particle i is far from the charged particle. In evaluating the linear term for large distances the dominant contribution to the sum is from screening particles j which at large separations are uncorrelated with either the charged particle or the particle i . Thus,

$$\vec{E}_i = \frac{q\vec{r}_{i0}}{r_{i0}^3} \left[1 - \frac{8\pi}{3} \rho \alpha \right] + O(\alpha^2), \quad (4)$$

independent of the detailed nature of the forces. The term in brackets is the asymptotic value of the screening function $S(r)$ to first order in the polarizability. Continuum theory predicts the screening as the usual $1/\epsilon$, modified by a cavity-field correction because the field is evaluated at the center of a particle. Since a particle in continuum theory is considered as being contained in

a cavity,

$$S = \frac{1}{\epsilon} \frac{3\epsilon}{2\epsilon + 1}. \quad (5)$$

This expression for S may be expanded by using the Clausius-Mosotti equation⁵

$$(\epsilon - 1)/(\epsilon + 2) = (4\pi/3)\rho\alpha + O(\alpha^3) \quad (6)$$

to show the equivalence^{6,7} to Eq. (4) to linear order:

$$S = 1 - (8\pi/3)\rho\alpha + O(\alpha^2). \quad (7)$$

The deviation between the continuum theory and the exact screening function due to differences in the nonlinear terms is evident from Fig. 1.

The ratio of the average electric field at a particle to the unscreened Coulomb field, $S(r)$, is shown in Fig. 1 to reach its asymptotic value about 3 molecular diameters away from the charge. This value is considerably higher than the continuum value (shown in Fig. 1 by a horizontal line) for a value of the polarizability $\alpha/\sigma^3 = 0.1$, somewhat higher than the value for argon of $\alpha/\sigma^3 = 0.04$. In these calculations periodic boundary conditions were used; however, none of the image particles was charged or polarized. The polarization was confined to the largest

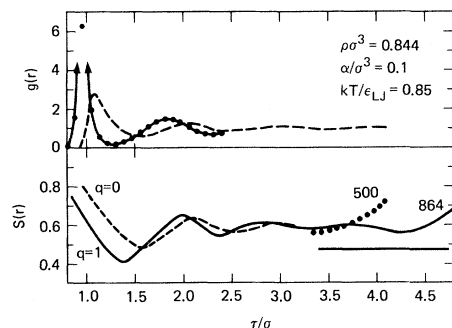


FIG. 1. Comparison of the radial distribution function, $g(r)$, and the screening function, $S(r)$, around a charged particle (solid line) and an uncharged particle (dashed line) near the triple point of Argon. The first peak of the radial distribution function around the charged particle is not sketched in because of lack of spatial resolution. The screening function for the charged system (solid line) is for a system of 864 particles. The same function calculated for a system of 500 particles is shown for large r/σ (dotted) to illustrate boundary effects. The horizontal solid line is the screening predicted by continuum dielectric theory using the Clausius-Mosotti value for the dielectric constant.

sphere in the central periodic cell centered on the charged particle. The effect of these boundary conditions on the screening function is seen in Fig. 1 by comparing the results for two different-sized systems. At small distances ($r/\sigma \lesssim 3.25$) the two systems gave essentially identical screening functions. The same slight decrease and then linear increase in the screening function near the boundary, beyond where the function reaches its asymptotic value, is also reproduced by a simple evaluation of the linear term in Eq. (3). The size system used here is thus sufficient to determine the asymptotic value. Also noteworthy about the screening function is that at distances as close as that of the nearest neighbors the field is already reduced to $\sim 70\%$ of the pure Coulomb-field value due to the induced polarization in the neighbors. The oscillations in the screening function follow quite closely the structural features in the radial distribution function shown in Fig. 1. The screening function around a charge in the limit $q \rightarrow 0$ is also shown on Fig. 1 and differs at small r from the $S(r)$ for $q = 1$. The two $S(r)$ curves have the same large- r behavior with both approaching a constant value of 0.59 ± 0.02 , where the estimate of the possible error is based on an examination of the r results for all q values listed in Table I.

Comparison of the radial distribution functions around the charged and uncharged particle show that the strong attractive force of the charge on the polarizable particles leads to the formation of a tightly packed solvation shell. The infrequent transfer of particles between the solvation shell and the rest of the fluid is indicated by the near-zero value of the radial distribution function at the first minimum. The average number of particles in the region within this first minimum decreases as the charge is increased. There are 12.5 particles on the average in that region for the uncharged system, 10.5 for a system with a charge of one-half electron unit, 9.5 for the singly charged system, and 8.5 for the 1.5-electron-unit charged system. This decrease represents the balance between the repulsed forces among the particles that are drawn in and their attractive force with the charge. For a doubly charged ion, the number of nearest neighbors decreases still further and there is evidence that a second shell of neighbors is significantly attracted to the charge.

An attempt to integrate the difference between the radial distribution function for the charged and uncharged system to obtain the partial molar

TABLE I. The free energy and diffusion constant of the charged particle in an argonlike fluid near the triple point. $\rho\sigma^3=0.844$, $kT/\epsilon_{LJ}=0.85$, $\alpha/\sigma^3=0.1$, $\alpha=3.4 \text{ \AA}$, $\epsilon_{LJ}/k=120^\circ$.

q	$-\frac{\partial(F/kT)^a}{\partial q}$	$-\frac{\Delta F}{kT}$	$\frac{R^b}{\sigma}$	$100D^{*c}$	D_0/D
0	4.1	1
0.25	108(18)	13	0.71	4.2	1
0.5	234(36)	55	0.68	3.5	1.2
0.75	380(54)	130	0.65	2.4	1.7
1.0	551(73)	246	0.61	1.7	2.4
1.0 ^d	547(61)				
1.5	947(109)	635	0.53	1.4	2.9
2.0	1410(145)	1220	0.49	0.6	6.8

^aThe tail correction calculated with $g(r)=1$ and $S(r)=0.6$ is given in parentheses.

^bThese radii have been calculated from the change in the Helmholtz free energy; however, it might be more appropriate to use the change in internal energy, which would lead to radii about 20% larger than those given here.

^cThe estimated error in D is 10% with a larger uncertainty for the case $q=0.25$ due to the presence of the low-frequency ion-rattling mode.

^dAll calculations were for a 500-particle system except this system of 864 particles. Typically twenty to thirty thousand time steps were used in the averaging with an energy conservation of about 1 part in 10^5 .

volume of the ion in solution⁸ unfortunately failed, because the integrated difference did not approach a limit but still oscillated at the largest distances due to the inward shift of the peaks of the radial distribution function for the charged system. To overcome this problem it would be necessary to use systems sufficiently large that structural differences between the two systems disappear before the boundary. Then, however, the partial molar volume would be a small difference of two large numbers and it is doubtful that a reliable result can be obtained by this method.

No difficulty was encountered in using the Onsager charging process to calculate the free energy of the ion in solution. The free-energy change, ΔF , upon charging the particle is obtained by integrating

$$\begin{aligned} \frac{\partial F}{\partial q} &= \left\langle \frac{\partial U}{\partial q} \right\rangle \\ &= - \left\langle \sum_i \vec{p}_i \cdot \frac{\vec{r}_{i0}}{r_{i0}^3} \right\rangle = -4\pi\rho\alpha q \int \frac{g(r)S(r)}{r^2} dr, \end{aligned} \quad (8)$$

where the angular brackets indicate statistical-

mechanical averaging. The result thus calculated is to be compared with the continuum model for the work involved in introducing a charged sphere of radius R in a uniform dielectric¹

$$\Delta F = -(1 - \epsilon^{-1})q^2/2R. \quad (9)$$

The results in Table I are given in terms of the radius required in the continuum expression to give the correct result. The radii are almost half the value of the nearest-neighbor distance which one would have expected to be the appropriate value for R . Even at small values of q , where the fluid structure is not as distorted, the radii are still considerably less than the nearest-neighbor distance.

To obtain the diffusion coefficient, the velocity autocorrelation function of the charged particle was computed for several values of the charge. Some cosine transforms,

$$f(\omega) = \left(\frac{\epsilon_{LJ}}{m\sigma^2} \right)^{1/2} \int \frac{\langle v(t)v(0) \rangle}{\langle v^2 \rangle} \cos\omega t dt, \quad (10)$$

are shown in Fig. 2. $f(\omega)$ is seen to develop a

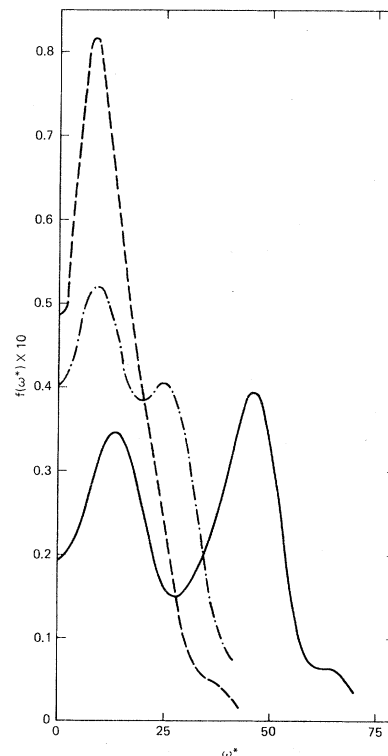


FIG. 2. Comparison of the cosine transform of the velocity autocorrelation function for an uncharged particle (dashed curve), charged particle (solid curve), and half-charged particle (dotted-dash curve).

peak at large values of $\omega^* = (m\sigma^2/\epsilon_{LJ})^{1/2}\omega$ which shifts to higher frequency as the charge increases. This mode can be identified as the vibration of the charged particle within the increasingly bound solvation shell. A crude harmonic model in which the solvation shell has been localized in a spherical shell at the first peak in the radial distribution function reproduces these peak frequencies rather well. The lower-frequency peak, present even in the uncharged system, can be attributed to backscattering of the diffusing particle in these dense systems. The shift in this lower-frequency mode as the charge increases could be due to backscattering of the ion and its solvation shell.

The diffusion constant, D , given by

$$D^* = (m/\epsilon_{LJ}\sigma^2)^{1/2}D = (kT/\epsilon_{LJ})f(0) \quad (11)$$

is presented in Table I and shows a decrease as the solvation shell forms around the charge. The diffusion coefficient of a sphere in a fluid, according to the Stokes-Einstein hydrodynamic theory, is inversely proportional to the sphere radius and fluid viscosity. Assuming the solvent viscosity is not affected by the charging process and that the same combination of stick or slip boundary conditions apply at the sphere surface for the charged and uncharged system, the ratio of the diffusion constant for the charged system to that of the uncharged system tells how the effective radius of the diffusing particle changes. If the ion and nearest neighbors diffuse as a unit, this ratio should be roughly 3. The actual ratio, given in the last column of Table I, is close to

1 for charges less than half an electron charge and then increases rapidly to a value near 3 for charges from 1 to 1.5 electron charges. For larger charges, the ratio further increase and it appears difficult to accurately predict a diffusion constant from a hydrodynamic model treating the ion and solvation shell as a unit.

We thank Mary Ann Mansigh for computational assistance. This work was performed under the auspices of the U. S. Department of Energy by the Lawrence Livermore Laboratory under Contract No. W-7405-ENG-48.

¹M. Born, *Z. Phys.* **1**, 45 (1920).

²S. A. Rice and P. Gray, *The Statistical Mechanics of Simple Liquids* (Interscience, New York, 1965).

³J. B. Hubbard and L. Onsager, *J. Chem. Phys.* **67**, 4850 (1977).

⁴P. G. Wolynes, *J. Chem. Phys.* **68**, 473 (1978).

⁵The α^3 term was shown to be small for Lennard-Jones systems in B. J. Alder, H. L. Strauss, and J. J. Weis, *J. Chem. Phys.* **62**, 2328 (1975).

⁶In an earlier paper for a permanent dipole in a polarizable fluid [E. L. Pollock and B. J. Alder, *Phys. Rev. Lett.* **39**, 299 (1977)], this cavity-field correction was left out and led to the erroneous conclusion that the continuum theory was incorrect for the term linear in the polarizability. Numerically this correction was near unity and the general conclusion of that paper regarding differences between the exact and the continuum-theory screening function remains valid.

⁷R. L. Fulton, *Phys. Rev. A* (to be published).

⁸J. G. Kirkwood and F. P. Buff, *J. Chem. Phys.* **19**, 774 (1951).

Superconducting Transition-Temperature Widths in Neutron-Irradiated Single-Crystal V₃Si

R. Viswanathan, R. Caton, and C. S. Pande

Brookhaven National Laboratory, Upton, New York 11973

(Received 22 March 1978; revised manuscript received 20 July 1978)

The superconducting transition temperature T_c and its width ΔT_c were determined for neutron-irradiated V₃Si for various fluences ϕt , using heat-capacity and resistivity measurements. It was found that, although the two determinations do not give identical results, in both cases ΔT_c increases with fluence indicating the inhomogeneous nature of the damage.

High-energy nuclear irradiation shows striking depressions in transition temperatures, T_c , of superconducting A15 compounds.¹⁻⁵ The mechanism of this depression is still a matter of some debate.⁶ Appel⁷ has given a theory of the radiation damage in these compounds assuming the

disorder to be antisite defects distributed homogeneously on the atomic scale. On the other hand, Pande⁸ has offered an alternative model in which the damage is taken to be in the form of small coherent disordered regions in a much less disordered matrix. Experimental evidence for this